Binding Properties of $Cu^{+/2+}$-(glycyl)$_n$glycine Complexes ($n = 1-3$)

Albert Rimola, Erika Constantino, Luis Rodríguez-Santiago,* and Mariona Sodupe*

Departament de Química, Universitat Autònoma de Barcelona, Bellaterra 08193, Spain

Received: November 26, 2007; In Final Form: January 11, 2008

The structure, relative energies, and binding energies of the complexes formed by the interaction of Cu^+ (d^{10},^{1}S) and Cu^{2+} (d^9,^{2}D) cations with the (glycyl)$_n$glycine ($n = 1-3$) oligomers have been theoretically determined by means of density functional methods. The most stable structures of the Cu^+ systems present linear dicoordination geometries, in agreement with a recent X-ray absorption spectroscopic study of Cu(I) interacting with model dipeptides. This is attributed to an efficient reduction of metal−ligand repulsion through sd σ hybridization in dicoordinated linear structures. In contrast, for Cu^{2+} systems the lowest energy structures are tricoordinated ($n = 1$), tetracoordinated ($n = 2$), and pentacoordinated ($n = 3$). For both copper cations, binding energy values show that the interaction energies increase when the peptide chain is elongated. Differences on the coordination properties of the ligands are discussed according to their length as well as to the electronic configuration of the metal cations, which are compared to the $Cu^{+/2+}$-glycine systems.

Introduction

The area of gas-phase chemistry has experienced considerable growth during the last decades due to its importance in proteomics and biochemistry.[1] Indeed, the knowledge of metal cation binding sites to peptides may not only be relevant in designing new strategies for peptide sequencing but also to get fundamental information of metalloproteins. The study of these systems in the gas phase allows obtaining information on their intrinsic chemical and physical properties, i.e., without complicating factors such as solvation or ion-pairing effects, of more complicated systems of biological importance. Mass spectrometry (MS) techniques are very valuable for the study of the interactions of metal cation−biomolecule complexes in the gas phase. Moreover, quantum chemical methods are nowadays a very useful tool to rationalize the results obtained in mass spectrometry experiments. Theoretical methods can accurately describe the metal ion complexes and supply relevant information such as the preferred metal coordination environment, metal cation affinities or trends on the nature of the bonding as a function of the metal cation configuration.

Of particular interest is the study of the interaction of Cu^+-(d^{10},^{1}S) and Cu^{2+}(d^9,^{2}D) cations with peptides since they are essential in a large number of biochemical processes.[2,3] Because of that, in recent years both experimental[4,5] and theoretical studies[6−8] have been performed to investigate the interaction of Cu^+ and Cu^{2+} with some peptide models. For Cu(I) interacting with model dipeptides, a recent X-ray absorption spectroscopic study has shown that the obtained complexes afford near linear two-coordinated structures.[9] In contrast, Cu-(II) tends to form structures with higher coordination numbers.[10]

Polyglycines can be considered as the backbone of peptides, so the use of glycine oligomers as models is a logical choice for initial studies to analyze the interaction of copper cations with peptides. In this sense, a great number of theoretical works (sometimes in combination with MS experiments) concerning the interaction of small polypeptides with alkali and transition metal cations have been reported in the literature.[6,7,11−23] Particularly interesting is the study of Shoeib et al., which compares the Cu(I) and Ag(I) complexes of glycine, diglycine, and triglycine, and shows that the coordination properties strongly depend on the nature of the metal cation. In particular, Cu^+ complexes were found to be always dicoordinated, whereas Ag^+ complexes were tri- and tetracoordinated.[21] In addition, we have recently presented a study that focuses on the interaction of glycylglycine with Cu^+, Ni^+, and Co^+.[17] Results showed that the most stable structure of the Cu^+-glycylglycine isomer is dicoordinated with the terminal carbonyl oxygen and the amino group attached to the metal. However, for the other two systems the lowest energy structures are tricoordinated, and the metal cation interacts with the same groups of Cu^+-glycylglycine plus the nickel (Ni^+-glycylglycine) or oxygen (Co^+-glycylglycine) atoms of the peptide bond, which points out the importance of the electronic configuration of the metal cation. It is thus interesting to analyze the differences on the coordination properties of Cu^+(d^{10}) and Cu^{2+}(d^9) due to both the electronic configuration of the metal cation and the elongation of the peptide chain. To the best of our knowledge a study on the interaction of Cu^{2+} with (glycyl)$_n$glycine ($n = 1-3$) have not been reported yet and with the present work we expect to provide new insights on the behavior of the backbone of peptides in front of these copper cations.

Methods

Full geometry optimizations and harmonic frequency calculations for different isomers of $Cu^{+/2+}$-(glycyl)$_n$glycine ($n = 1-3$) have been performed by means of density functional theory (DFT) calculations. DFT methods have been widely used to study transition-metal-containing systems, and it has been shown that the B3LYP approach is a cost-effective method for studying this kind of systems.[24,25] However, for Cu^{2+}−ligand systems, recent studies carried out in our group have demonstrated that functionals with a different percentage of exact exchange can provide different results when the degree of charge and spin delocalization is important.[26−28] It was found that delocalized situations are overstabilized by some functionals (LDA, GGA,

* To whom correspondence should be addressed. E-mail: luis@klingon.uab.es (L.R.-S.); Mariona.Sodupe@uab.es (M.S.).

10.1021/jp711189s CCC: $40.75
Published on Web 03/06/2008

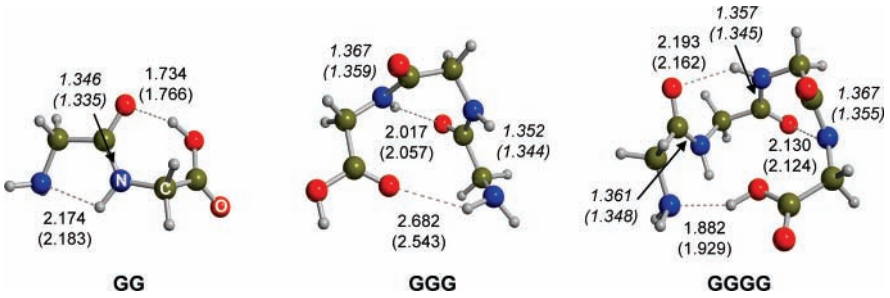

Figure 1. B3LYP (BHLYP)-optimized geometries of the most stable conformers of GG, GGG, and GGGG systems. Distances are in angstroms.

and also B3LYP) as a result of a bad cancellation of the self-interaction part by the exchange-correlation functional.[29] The admixture of exact exchange, which rigorously corrects the self-interaction, reduces the error. The results suggest that the most proper mixture of exact exchange is given by the hybrid exchange Becke's half-and-half functional.[26−28] Therefore, the structures of Cu^+-(glycyl)$_n$glycine systems have been obtained using the nonlocal hybrid three-parameter B3LYP[30,31] density functional approach, whereas for the Cu^{2+}-containing ones, results have been obtained both with the B3LYP and BHLYP[31,32] methods. In addition, and to evaluate the reliability of the DFT results, for Cu^{2+}-glycylglycine systems we have also performed single-point CCSD(T)[33] energy calculations both at the B3LYP- and BHLYP-optimized geometries.

To explore the conformational space of this kind of systems, a previous conformational search of the Li^+-(glycyl)$_n$glycine ($n = 1-3$) complexes has been done to model the electrostatic interaction of the metal cation with the polyglycines. This primary study has been carried out using the Monte Carlo Multiple Minimum (MCMM) procedure,[34] with the AMBER* force field,[35,36] as implemented in the Macromodel 7.0 package.[37] In these calculations we have considered both the neutral form of the peptides as well as different zwitterionic forms (with NH_3^+ amino moiety or COH^+ amide groups). Among all the possible structures obtained, only those lying within a range of 10 kcal mol^{-1} have been calculated at the DFT level. Moreover, some structures not obtained in this initial conformational search but chemically important and derived from experience and chemical intuition have also been computed.

The following basis set was used. For Cu we employed the Watcher's primitive basis set (14s9p5d),[38] supplemented with one s, two p, and one d diffuse functions,[39] plus one f polarization function, the final basis set being (15s11p6d1f)/[10s7p4d1f]. For C, N, O, and H we used the standard 6-31++G(d,p) basis set.

All density functional calculations have been performed using the Gaussian 03 set of programs package.[40] Open-shell calculations were based on an unrestricted formalism. Thermodynamic corrections were obtained assuming an ideal gas, unscaled harmonic vibrational frequencies, and the rigid rotor approximation by standard statistical methods.[41] Electron spin densities and net atomic charges on the atoms were obtained using the population analysis of Weinhold et al.[42]

Transition metal cation−ligand binding energy can be decomposed in different terms; the main ones being: the deformation energy of the ligand when coordinating to the metal cation, the electrostatic interaction, the metal−ligand repulsion, and the charge transfer, which reflects the electronic delocalization between the metal and the ligand. In this work, to get a deeper insight on the nature of the bonding between Cu^+ and the glycine oligomers, the interaction energies of the most stable isomers have been computed in two steps at B3LYP/6-31++G(d,p). First, the deformation energy (E_{def}) of polyglycines was calculated by determining the energy difference between the polyglycines at the geometries of the complexes and the free polyglycines in their respective ground-state conformers. Second, the electrostatic interaction (E_{elec}) has been calculated by the energy lowering of the deformed polyglycines in the presence of a single-point charge replacing the cation. In this calculation the electronic relaxation of the ligands is allowed and, thus, it also includes the polarization term. The sum of $E_{def} + E_{elec}$ gives us the interaction energy between polyglycines and a point charge ($\Delta E_{int(pc)}$).

Results and Discussion

Results are organized in three sections. The first two show the structure and relative energies of the different Cu^+ and Cu^{2+} systems, respectively. In the last section, the binding energies of each system and the trends observed upon elongating the chain are discussed. For the sake of brevity, the glycylglycine, the glycylglycylglycine, and the glycylglycylglycylglycine peptides will be designated hereafter as GG, GGG, and GGGG, respectively. In addition, the nitrogen atom of the terminal amino group will be referred as **N**, the oxygens and nitrogens of the peptide bond as $\mathbf{O_{pn}}$ and $\mathbf{N_{pn}}$, respectively, where **n** is the number of the peptide bond starting from the NH_2 terminus, the terminal oxygen of the carbonyl group as **O**, and the oxygen of the hydroxyl group as $\mathbf{O_H}$.

Figure 1 shows the global B3LYP and BHLYP minima of the neutral forms of GG, GGG, and GGGG systems, which have been located after considering the most stable and significant structures arising from previous Monte Carlo and DFT calculations. The GG conformer has been described recently as the most stable form.[43] For the GGG and GGGG cases, other conformations were found close in energy (within a range of 1 kcal mol^{-1}). However, since the energy difference between them is very small, $Cu^{+/2+}$ binding energies will not be substantially be influenced whether we consider one structure or another.

Cu^+-GG, -GGG, -GGGG. The B3LYP-optimized geometries, the main metal−ligand distances, and the relative potential energies including the ZPE (ΔU_0) for the Cu^+-GG, Cu^+-GGG, and Cu^+-GGGG systems are given in Figure 2, Figure 3, and Figure 4, respectively.

As described in a previous work,[17] the most stable isomer of the Cu^+-GG system corresponds to **Cu^+-GG1**, where Cu^+ is coordinated to the terminal amino (**N**) and carbonyl oxygen (**O**). When Cu^+ interacts with the GGG peptide, the ground-state isomer presents also an almost linear dicoordination where the $\mathbf{O_{p1}}$ and the **O** atoms are the donor atoms (**Cu^+-GGG1**), as found previously by Shoeib et al.[21] Finally, the most stable isomer of the Cu^+-GGGG system (**Cu^+-GGGG1**) is also dicoordinated, the Cu^+ cation interacting with the $\mathbf{O_{p1}}$ and $\mathbf{O_{p3}}$ donor centers. Therefore, the trend is clear: Cu^+ prefers to be chelated by two atoms with a coordination angle close to 180°, even in the case of the larger peptide studied where several basic

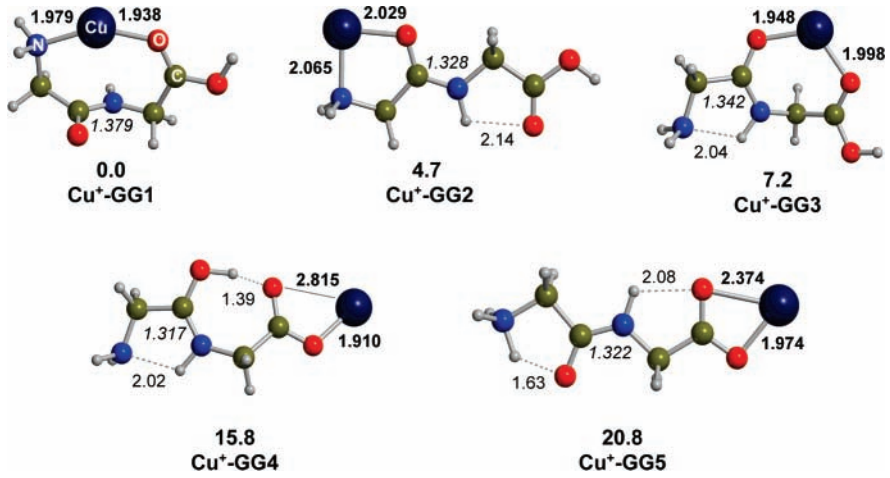

Figure 2. B3LYP-optimized geometries of the Cu^+-GG isomers. Relative potential energies including the ZPE values, in kcal mol^{-1}. Distances are in angstroms.

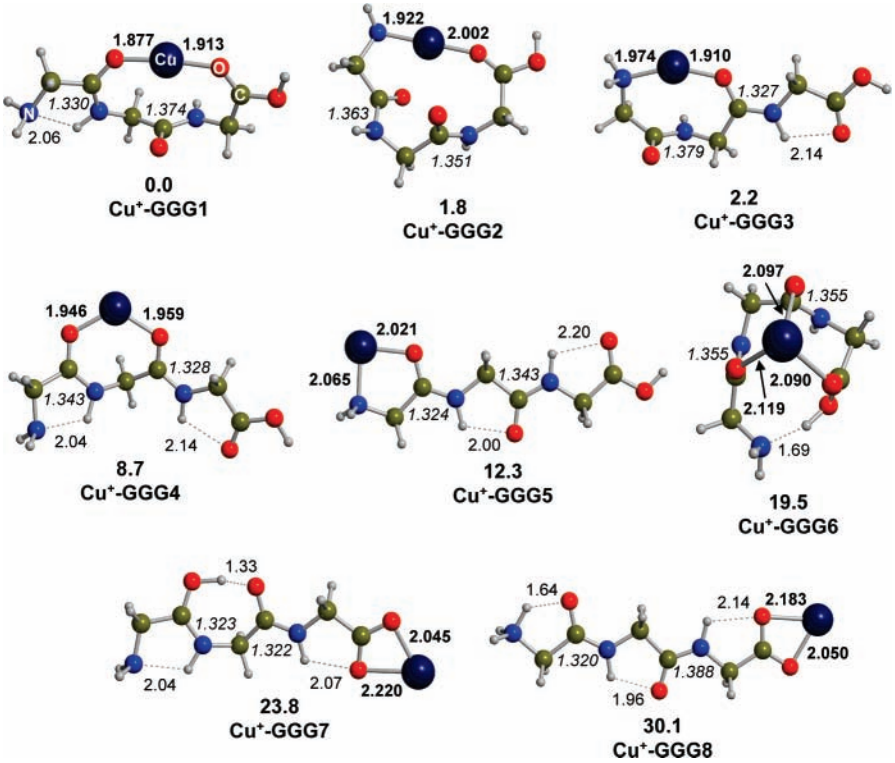

Figure 3. B3LYP-optimized geometries of the Cu^+-GGG isomers. Relative potential energies including the ZPE values, in kcal mol^{-1}. Distances are in angstroms.

groups are available. This is in agreement with a recent experimental study on His dipeptides, which shows the predominance of linear two-coordinated geometry.[9] This trend is reinforced by the fact that the second and the third most stable forms of Cu^+-GGG and Cu^+-GGGG present also this same way of coordination (**Cu^+-GGG2** and **Cu^+-GGG3** are 1.8 and 2.2 kcal mol^{-1} higher in energy than **Cu^+-GGG1**, respectively, and **Cu^+-GGGG2** and **Cu^+-GGGG3** lie 0.2 and 1.5 kcal mol^{-1} above **Cu^+-GGGG1**, respectively). The mechanism of interaction of these structures is well-known. By assumption of *z* as the binding axis, the highest d orbital of Cu^+ is the d_{z^2} one, which is hybridized with the 4s orbital in order to reduce the repulsion along the metal−ligand axis and on both sides of Cu^+ at the same time. In this way, the cost of the sd_{z^2} hybridization is shared by the interaction with the two basics sites. However, when an additional basic site of the backbone enters in the coordination sphere, it is impossible to arrange them in a fashion that all of them benefit from sd_{z^2} hybridization, and consequently, the coordination of a third donor center becomes unfavorable.

In Cu^+-glycine system,[44] the most stable isomer is that in which the **N** and the **O** atoms coordinate to the metal cation forming a five-membered ring. Similar structures have been found in the present work (**Cu^+-GG2**, **Cu^+-GGG5**, and **Cu^+-GGGG7**), but lying 4.7, 12.3, and 18.3 kcal mol^{-1} above the corresponding most stable isomers, respectively. It can be noted that the relative energy of these forms increases as the peptide chain is elongated, and thus, the coordination mode of the most stable isomer of Cu^+-glycine system becomes disfavored. These results indicate that the Cu^+ cation prefers a linear coordination environment rather than an angular coordination. The reason is that in order to reduce the Pauli repulsion between the metal cation and the ligand in a linear coordination, the d_{z^2} orbital of the metal cation hybridizes with the 4*s* one, whereas in the

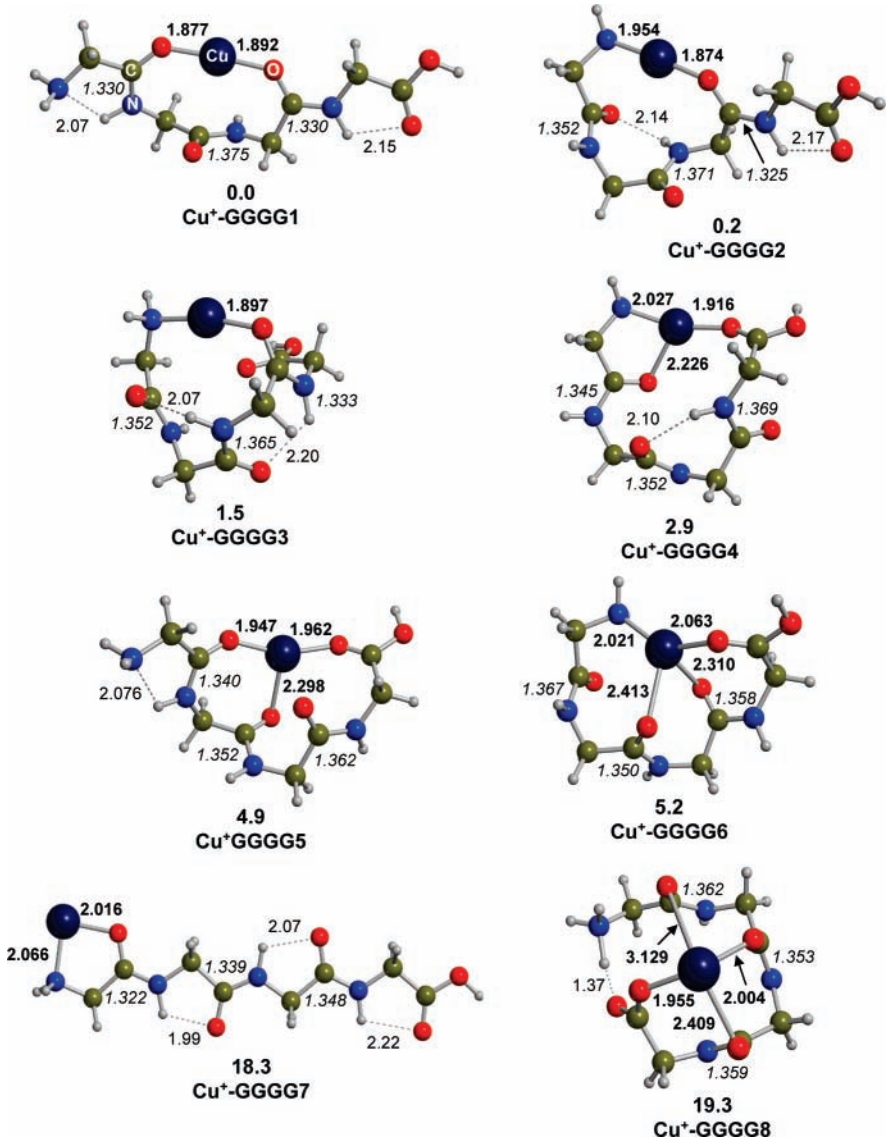

Figure 4. B3LYP-optimized geometries of the Cu^+-GGGG isomers. Relative potential energies including the ZPE values, in kcal mol^{-1}. Distances are in angstroms.

angular coordination this is produced through the d_{xz} and 4p hybridization. Since the 4p orbitals lie higher in energy than the 4s one, the hybridization is less effective in angular coordination structures, and thus, the repulsion minimization is smaller, giving rise to more unstable structures. For Cu^+-glycine the most stable isomer follows an angular geometry because it is not possible to establish a linear coordination due to geometry restrictions.

Cu^+-GG3 and **Cu^+-GGG4** are dicoordinated structures, in which the metal cation interacts with two neighbor carbonyl oxygens: the **O_{p1}** and **O** atoms and the **O_{p1}** and **O_{p2}** atoms, respectively. In these cases the coordination angle is close to 150°. These structures are quite stable compared to the respective ground-state isomer (7.2 and 8.7 kcal mol^{-1} higher in energy). However, if only charge-solvated forms are taken into account, structures with this kind of coordination do not exist in Cu^+-GGGG. Instead, other more coordinated species are observed, such as the tricoordinated **Cu^+-GGGG5** and the tetracoordinated **Cu^+-GGGG6**, which lie 4.9 and 5.2 kcal mol^{-1} above **Cu^+-GGGG1**, respectively. Therefore, as the number of donor atoms is increased, the metal cation tends to be coordinated by more than two donor atoms. However, this increment on the cation environment does not imply a loss of the preference of Cu^+ to follow linear coordination.

Finally, the zwitterionic forms located deserve to be commented. For Cu^+-GG, two zwitterionic forms have been found: one in which the **O_{p1}** atom is protonated (**Cu^+-GG4**) and another one where the **N** atom is protonated (**Cu^+-GG5**). These two structures are the most unstable ones of the Cu^+-GG system (15.8 and 20.8 kcal mol^{-1} higher in energy than the **Cu^+-GG1** isomer, respectively). A similar behavior is observed for Cu^+-GGG, for which two zwitterionic forms have also located (**Cu^+-GGG7** with the protonated **O_{p1}** atom and **Cu^+-GGG8**, where protonation takes place at the **N** atom). Once again, these two structures are the most unstable ones (23.8 and 30.1 kcal mol^{-1} above the **Cu^+-GGG1** isomer, respectively). In addition, the zwitterionic form in which the proton is on the **O_{p2}** atom (not reported here) has also been identified and lies around 37 kcal mol^{-1} with respect to the **Cu^+-GGG1** isomer. Finally, the only zwitterionic form found for Cu^+-GGGG (**Cu^+-GGGG8**), which remains 19.3 kcal mol^{-1} above the most stable isomer, is that in which the metal cation is tetracoordinated through the **O_{p1}**, **O_{p2}**, **O_{p3}**, and **O** atoms, while the amino group has received the proton from the hydroxyl group. In summary,

TABLE 1: Contributions to the Total Interaction Energy (in kcal mol^{-1}) for the Four Most Stable Isomers of Cu^+-GG, -GGG, and -GGGG Systems, Computed at B3LYP/6-31++G(d,p)

Cu^+-G_mX	E_{def}	E_{elec}	$\Delta E_{int(pc)}$[a]	$\Delta E_{rel(pc)}$[b]	ΔE_{int}[c]	ΔE_{rel}[d]
GG1	12.6	−108.7	−96.1	0.0	−87.5	0.0
GG2	10.1	−102.0	−91.9	4.2	−82.4	5.1
GG3	10.4	−100.2	−89.8	6.3	−79.6	7.9
GG4	17.8	−92.7	−74.9	21.2	−69.9	17.6
GGG1	13.7	−118.1	−104.4	0.0	−97.1	0.0
GGG2	21.9	−123.8	−101.9	2.5	−96.2	0.9
GGG3	16.0	−121.5	−105.5	−1.1	−95.6	1.5
GGG4	13.7	−114.1	−100.7	3.7	−88.5	8.6
GGGG1	16.6	−129.5	−112.9	0.3	−104.7	1.3
GGGG2	15.8	−129.0	−113.2	0.0	−106.1	0.0
GGGG3	14.0	−127.0	−113.0	0.2	−105.1	0.9
GGGG4	23.9	−133.4	−109.5	3.7	−103.0	3.0

[a] $\Delta E_{int(pc)}$ = interaction energies of (+)-glycine oligomers: $E_{def} + E_{elec}$. [b] $\Delta E_{rel(pc)}$ = relative energies considering $\Delta E_{int(pc)}$. [c] ΔE_{int} = interaction energy of (Cu^+)-glycine oligomers of the selected isomers. [d] ΔE_{rel} = relative energies considering ΔE_{int}.

the zwitterionic forms of the Cu^+-GG, Cu^+-GGG, and Cu^+-GGGG systems are the most unstable isomers of the explored potential energy surfaces.

As aforementioned, several factors can determine the relative stability of these structures. To shed light on the nature of bonding of the Cu^+ complexes, Table 1 reports the deformation energy (E_{def}) of polyglycines, the electrostatic interaction (E_{elec}) as well as the interaction of the ligands interacting with a single point charge ($E_{int(pc)}$). These terms have been computed following the procedure described in the Methods section for the four more stable isomers of Cu^+-GG, Cu^+-GGG, and Cu^+-GGGG. First, one can observe that the E_{def} term is positive and larger in longer peptide chains, whereas the E_{elec} is negative and larger as the peptide chain is increased. It is interesting to compare the relative energies obtained using a point charge ($\Delta E_{rel(pc)}$) model and those computed for the Cu^+-(glycyl)$_n$-glycine isomers (ΔE_{rel}). For the GG and GGGG cases, the relative energies follow the same trend but the obtained values are somewhat different. For the GGG complexes the relative order is not the same (according to the point charge model the most stable form should be GGG3), but the energy differences are small. These results point out that although the interaction of Cu^+ with polyglycines is mainly electrostatic, other factors such as Pauli repulsion or charge transfer, are also important in determining their stability.

Cu^{2+}-GG, -GGG, -GGGG. Figures 5−7show the B3LYP- and BHLYP-optimized geometries as well as their relative energies including the ZPE corrections of the structures located for the Cu^{2+}-GG, Cu^{2+}-GGG, and Cu^{2+}-GGGG systems, respectively.

Cu^{2+} is a doubly charged d^9 cation with one monooccupied d orbital. In these conditions, the repulsion between the metal and the ligand is smaller than for Cu^+ (a d^{10} cation) and the electrostatic interaction larger. Therefore, the interaction with more than two donor centers is expected to become more favorable.

In comparison of the B3LYP relative energies with those obtained with BHLYP, significant differences are observed. As a general trend, the relative energies computed with B3LYP are smaller than the BHLYP ones, especially for Cu^{2+}-GG and Cu^{2+}-GGG. Additionally, for the particular case of the Cu^{2+}-GG system, the ground-state isomer depends on the functional employed; that is, according to the B3LYP results the lowest energy structure is the salt bridge **Cu^{2+}-GG3**, whereas with BHLYP it corresponds to the charge-solvated **Cu^{2+}-GG1**. Furthermore, with the B3LYP method other more stable structures than **Cu^{2+}-GG1** are found (**Cu^{2+}-GG2** and **Cu^{2+}-GG4**). To shed some light to this intriguing differences we have carried out some single-point energy CCSD(T) calculations both upon the B3LYP- and BHLYP-optimized geometries of the different Cu^{2+}-GG isomers, the results summarized in Table 2. According to these CCSD(T) results, some observations are noticeable: (i) there are no important energy differences regardless of whether the single-point calculations are performed upon the B3LYP- or BHLYP-optimized geometries; (ii) **Cu^{2+}-GG2** is the most stable isomer, in contrast to what B3LYP or BHLYP methods suggest, which provide **Cu^{2+}-GG3** and **Cu^{2+}-GG1** as the most stable structure, respectively; (iii) overall, although BHLYP fails in determining the ground state isomer for Cu^{2+}-GG, the BHLYP relative energies compare better to the CCSD(T) results than the B3LYP ones, which are too small. As described in the literature,[26−29] functionals with different amounts of exact exchange mixing can show significant discrepancies when comparing situations with different spin distribution, since GGA or hybrid functionals with low percentages of exact exchange mixing overstabilize delocalized situations. Natural population analysis indicates that B3LYP provides more delocalized spin density situations than BHLYP. On the other hand, the less coordinated the metal cation is, the larger the delocalization of the spin density is; thus the peptide becomes partially oxidized. Consequently, it is not surprising that the relative energies corresponding to structures going from **Cu^{2+}GG3** to **Cu^{2+}GG6** are all too small at the B3LYP level, given that we are comparing dicoordinated and monocoordinated complexes (more spin delocalized and overstabilized by B3LYP) with tricoordinated ones (**Cu^{2+}-GG1** and **Cu^{2+}-GG2**), for which the spin density mainly lies at the metal cation. The failure of BHLYP to predict the most stable isomer of the Cu^{2+}-GG system does not seem to be related to the changes in spin density distribution since it is similar in both complexes. Probably it is a consequence of the subtle balance of many factors, arising from the different pyramidal vs T-shape coordination found for **Cu^{2+}-GG1** and **Cu^{2+}-GG2**, respectively, and to the small energy difference between them (see Table 2). For Cu^{2+}-GGG and Cu^{2+}-GGGG systems, however, both functionals provide the same ground-state structure and, except for a few cases, the same relative stabilities. Again, relative energies computed with B3LYP are smaller than the BHLYP ones, although the differences tend to decrease for highly coordinated systems, for which the spin density is almost completely located at the metal cation both at the B3LYP and BHLYP levels of theory.

These facts are consistent with what was previously exposed and described in the literature.[26−28] That is, with Cu^{2+}-coordinatively unsaturated species one must be careful with the functional to employ since the ligands are more prone to be oxidized and the spin distribution can change from one structure to another. In these cases, functionals with a larger amount of exact exchange than B3LYP, such as BHLYP, appear to compare better with CCSD(T). However, in situations in which the coordination environment of Cu^{2+} is saturated, the electron hole is located at the metal cation, and thus, both B3LYP and BHLYP behave similarly. Therefore, and in order to facilitate the discussion, hereafter we will refer to the BHLYP results.

As mentioned, the electronic configuration of the Cu^{2+} cation is a d^9,^{2}D electronic ground state and consequently, in contrast to the Cu^+(d^{10},^{1}S) metal cation, the coordination of more than two donor atoms is expected due to the smaller metal−ligand repulsion and larger electrostatic interaction. In fact, this is the case for the present systems: the most stable isomers found

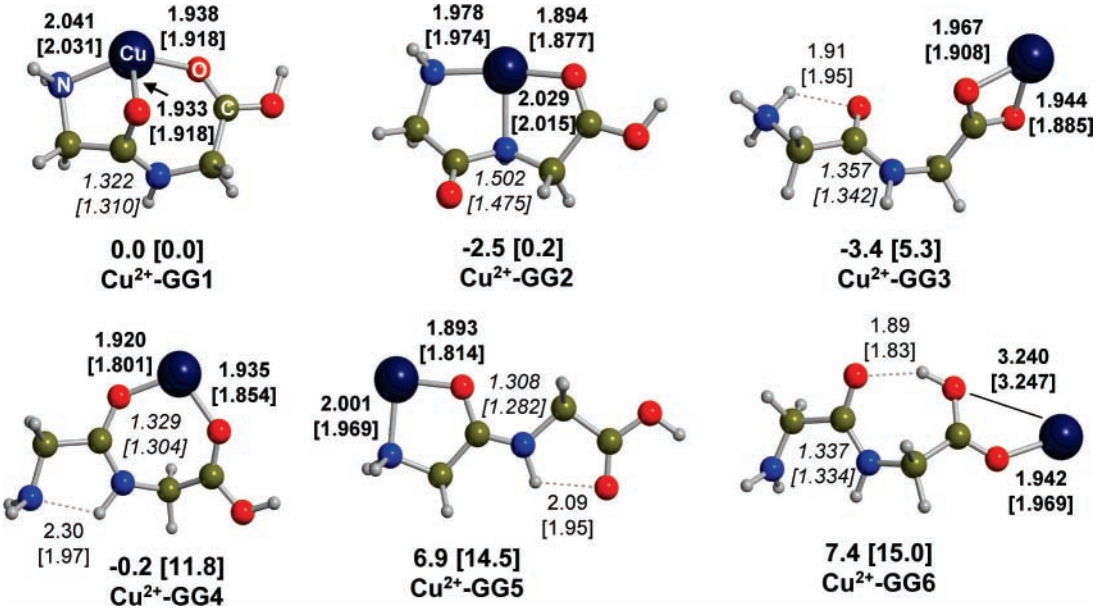

Figure 5. B3LYP [BHLYP]-optimized geometries of the Cu^{2+}-GG isomers. Relative potential energies including the ZPE values, in kcal mol^{-1}. Distances are in angstroms.

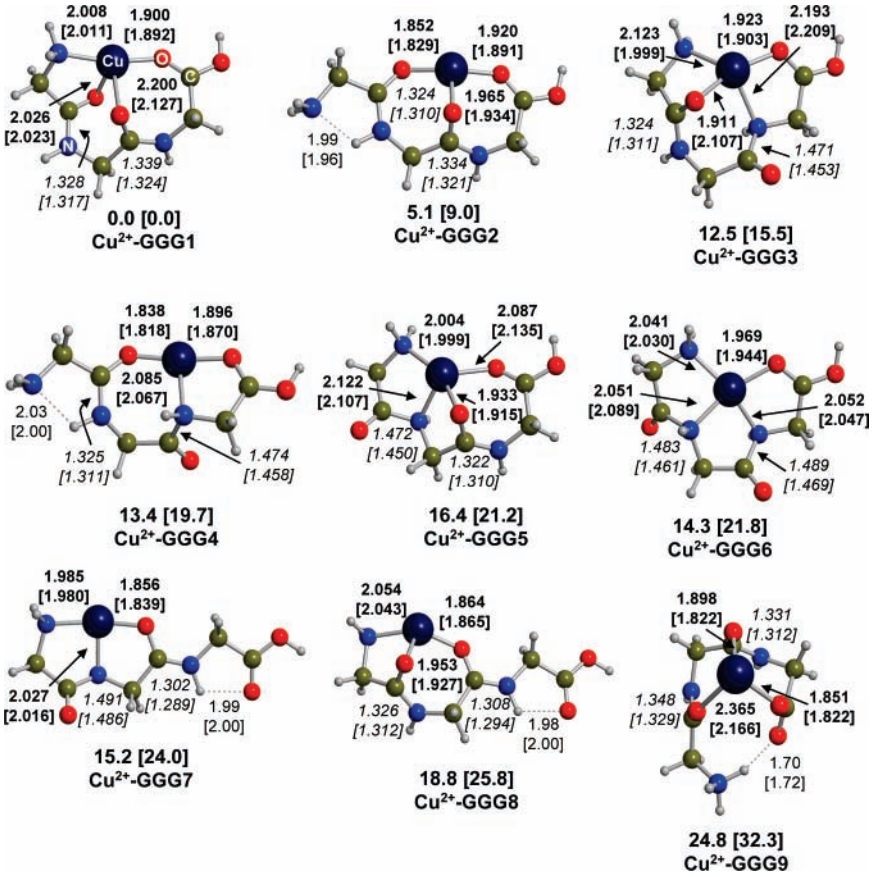

Figure 6. B3LYP [BHLYP]-optimized geometries of the Cu^{2+}-GGG isomers. Relative potential energies including the ZPE values, in kcal mol^{-1}. Distances are in angstroms.

for the three systems are tricoordinated (**Cu^{2+}-GG2**, see Figure 5 and Table 2), tetracoordinated (**Cu^{2+}-GGG1**, see Figure 6), and pentacoordinated (**Cu^{2+}-GGGG1**, see Figure 7), for which, in addition to the terminals **N** and **O** atoms, the nitrogen $\mathbf{N_p}$ or oxygen $\mathbf{O_p}$ of the peptide bonds take part of the coordination sphere.

The possibility that polyglycines coordinate through either the $\mathbf{O_{pn}}$ or the $\mathbf{N_{pn}}$ atoms was already observed in the Ni^{+}-GG and Co^{+}-GG systems, which was attributed to the electronic configuration of the metal,[17] and it is enhanced when the number of peptide bonds increases. For instance, in Cu^{2+}-GGG there are two peptide bonds that can interact with the Cu^{2+} cation leading to four different isomers, each one being tetracoordinated. These isomers are: **Cu^{2+}-GGG1**, **Cu^{2+}-GGG3**, **Cu^{2+}-GGG5**, and **Cu^{2+}-GGG6**. In all of them, two of the coordinating sites are the amino **N** and the carbonyl **O**. The other two are either the $\mathbf{N_p}$ or the $\mathbf{O_p}$ of the first and second peptide bonds. From the relative energies, it can be observed that structures

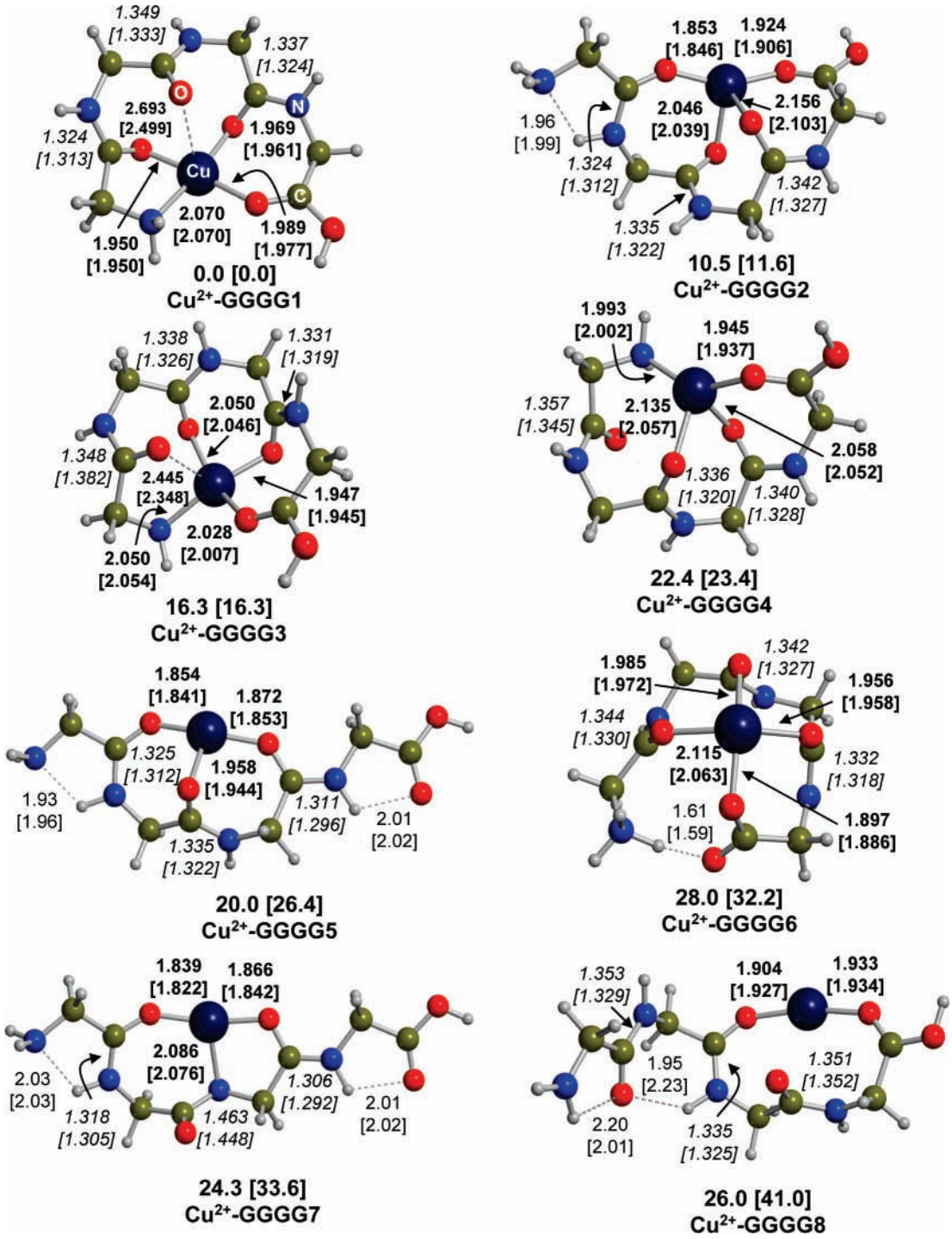

Figure 7. B3LYP [BHLYP]-optimized geometries of the Cu^{2+}-GGGG isomers. Relative potential energies including the ZPE values, in kcal mol^{-1}. Distances are in angstroms.

TABLE 2: Relative Electronic Energies Computed at B3LYP, BHLYP, CCSD(T)//B3LYP, and CCSD(T)//BHLYP, in kcal mol^{-1}

isomer	B3LYP	BHLYP	CCSD(T)//B3LYP	CCSD(T)//BHLYP
Cu^{2+}-GG1	0.0	0.0	0.0	0.0
Cu^{2+}-GG2	−2.1	0.5	−2.5	−2.6
Cu^{2+}-GG3	−2.4	6.3	3.6	3.0
Cu^{2+}-GG4	1.7	13.0	18.6	16.3
Cu^{2+}-GG5	8.0	15.1	17.7	16.0
Cu^{2+}-GG6	10.3	18.7	16.1	16.0

where Cu^{2+} interacts with $\mathbf{O_p}$ are generally preferred to those in which Cu^{2+} interacts with $\mathbf{N_p}$. Indeed, the most stable isomer (**Cu^{2+}-GGG1**) presents a **N**, $\mathbf{O_{p1}}$, $\mathbf{O_{p2}}$, **O** coordination, whereas **Cu^{2+}-GGG3**, **Cu^{2+}-GGG5**, and **Cu^{2+}-GGG6** show a **N**, $\mathbf{O_{p1}}$, $\mathbf{N_{p2}}$, **O**; a **N**, $\mathbf{N_{p1}}$, $\mathbf{O_{p2}}$, **O**; and a **N**, $\mathbf{N_{p1}}$, $\mathbf{N_{p2}}$, **O** coordination, which lie 15.5, 21.2, and 21.8 kcal mol^{-1} above the ground-state isomer, respectively. This may be due to the fact that Cu^{2+}-$\mathbf{O_p}$ interaction strengthens the peptide bond, contrarily to the Cu^{2+}-$\mathbf{N_p}$ binding that weakens this bond.

Nevertheless, in some cases the trend is not followed, as occurs in the already discussed **Cu^{2+}-GG1**/**Cu^{2+}-GG2** pair, which at the CCSD(T) level the latter one is more stable than the former one, or in the **Cu^{2+}-GGG7**/**Cu^{2+}-GGG8** pair, in which the former isomer (coordination through the **N**, $\mathbf{N_{p1}}$, $\mathbf{O_{p2}}$ atoms) is more stable than the latter one (coordination through the **N**, $\mathbf{O_{p1}}$, $\mathbf{O_{p2}}$ atoms). It should be noted, however, that in

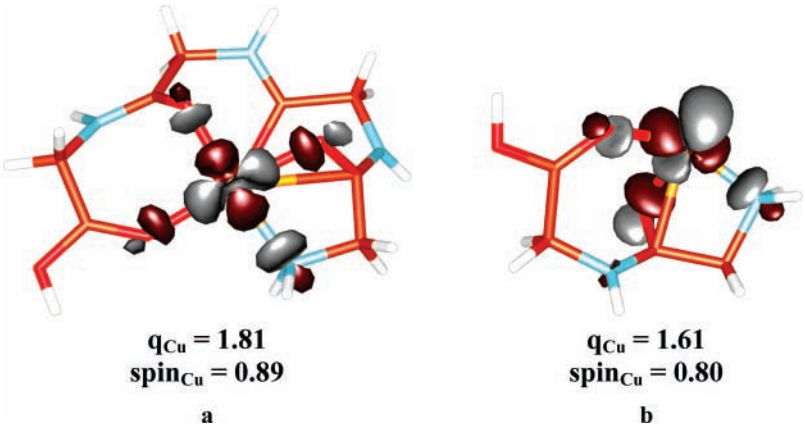

Figure 8. SOMO of the **Cu^{2+}-GGGG1** (a) and **Cu^{2+}-GG1** (b) isomers at BHLYP. The net charges (q_{Cu}) and the spin densities ($spin_{Cu}$) on the metal cation are also included.

these two latter cases the coordination environment upon interacting with $\mathbf{N_p}$ or $\mathbf{O_p}$ is somewhat different. When the metal cation interacts with $\mathbf{O_p}$ the complex adopts a tricoordinated pyramidal structure, whereas when it interacts with $\mathbf{N_p}$ the complex acquires a T-shaped coordination, where sd σ hybridization is more effective allowing shorter N−Cu and O−Cu bond lengths. Overall, these results show that the relative stability of the different coordination depends on several factors such as the different intrinsic metal affinity of each donor atom, the metal−ligand repulsion, or the peptide distortion energy as well.

Among the isomers of the Cu^{2+}-GGGG system, one can find dicoordinated, tricoordinated, tetracoordinated, and pentacoordinated structures, which enable us to establish the preferred coordination modes of the Cu^{2+} cation. The lowest and third most stable isomers are pentacoordinated (**Cu^{2+}-GGGG1** and **Cu^{2+}-GGGG3**, the relative energies being 0.0 and 16.3 kcal mol^{-1}, respectively) adopting a square pyramidal structure, whereas the second and fourth most stable isomers are tetracoordinated (**Cu^{2+}-GGGG2** and **Cu^{2+}-GGGG4**, lying 11.6 and 23.4 kcal mol^{-1} above **Cu^{2+}-GGGG1**, respectively), with a structure close to a distorted butterfly geometry. Among the charge solvated forms, there are two tricoordinated structures corresponding to **Cu^{2+}-GGGG5** and **Cu^{2+}-GGGG7**, 26.4 and 33.6 kcal mol^{-1} higher than **Cu^{2+}-GGGG1**, respectively, and one dicoordinated structure, **Cu^{2+}-GGGG8**, which lies 41.0 kcal mol^{-1} above the most stable one. In this last isomer the ligand has been oxidized by the metal cation (the spin density is located on the amine group, becoming more planar) and the metal becomes a Cu^+ monocation, which prefers, as aforementioned, to follow a linear dicoordination mode. In general, the coordination preferences are: pentacoordination > tetracoordination > tricoordination > dicoordination, although some exceptions may appear due to the deformation energy of the ligand or to geometry constraint effects that impose a certain coordination environment. Overall, from these results one may predict that a Cu^{2+} cation interacting with longer peptide chains would probably saturate its coordination environment with six donor atoms adopting a distorted octahedral geometry due to a Jahn−Teller effect.

It has been observed that the zwitterionic forms for Cu^+-polyglycines are the most unstable forms for each system. For Cu^{2+}-polyglycines, the salt bridge structures are not the most energetic isomers of the explored potential energy surfaces but as the peptide chain increases these forms become more unstable and remain quite high in energy with respect to the most stable ones. This is probably due to the fact that, upon enlarging the peptide, the Cu^{2+} becomes more coordinated in such a way that the electrostatic interaction is reduced by a significant screening effect. Obviously, the instability shown by the Cu^{2+} zwitterion isomers may be modified by solvent effects.

An interesting aspect to analyze is the spin density in these systems. Except for **Cu^{2+}-GG6** and **Cu^{2+}-GGGG8**, for which a total oxidation of the ligand is observed, for the remaining complexes the spin density values of the metal cation range around 0.60−0.80, 0.75−0.85, and 0.82−0.89 for the Cu^{2+}-GG, -GGG, and -GGGG systems, respectively. For Cu^{2+}-glycine,[44] the spin density at the metal cation ranged around 0.10−0.58. Therefore, there is a clear tendency: the longer the peptide chain is (and thus the larger the coordination to the metal cation), the smaller the oxidation of the ligand is. Similar facts were observed when Cu^{2+} cations interact with a guanine−cytosine base pair, since the degree of oxidation of the base pair was found to highly depend on the coordination environment of the metal cation.[45] These facts can be understood considering the metal−ligand interactions. **Cu^{2+}-GGGG1** shows a square-pyramidal structure with the **N**, $\mathbf{O_{p1}}$, $\mathbf{O_{p3}}$, and **O** atoms in the equatorial plane and $\mathbf{O_{p2}}$ in the apical site. The ligand in the equatorial plane (xy) largely destabilizes the $d_{x^2-y^2}$ orbital of the metal cation and thus, the preferred situation has this orbital mono-occupied (Figure 8a). However, for **Cu^{2+}-GG1**, with a trigonal-like disposition, the ligand field splitting is smaller than in the square-planar environment, and thus, 3d orbitals are less destabilized, which favors the spin delocalization on the ligand (Figure 8b). Thus, the oxidation induced by Cu^{2+} is related to the degree of coordination: the more coordinated the metal is, the less oxidized the ligand is. This point should not be overlooked since the $Cu^{+/2+}$ redox pair is involved in many important biochemical processes. In this sense, due to the fact that Cu(I) presents less coordinated structures than Cu(II), the reduction potential in protein copper sites is expected to raise compared to that of the aqueous $Cu^{+/2+}$ pair, due to a net stabilization of the less-charged Cu^+ oxidation state.[6]

Binding Energies of $Cu^{+/2+}$-GG, -GGG, -GGGG Systems. In Table 3 the computed D_e, D_0, ΔH^0_{298}, and ΔG^0_{298} values for the most stable $Cu^{+/2+}$-GG, -GGG, and -GGGG structures are reported. In addition, the calculated interaction energies of the $Cu^{+/2+}$-glycine systems are also shown.

For both metal cations, the binding energies increase as the peptide chain is elongated. In both cases this fact is related to a larger electrostatic interaction. Although for Cu^+ the most stable structures are always dicoordinated, they differ on their coordination angles, which are 90, 150, 180, and 180° for Cu^+-glycine,[44] **Cu^+-GG1**, **Cu^+-GGG1**, and **Cu^+-GGGG1**, respec-

TABLE 3: Binding Energies (D_e, D_0, ΔH^0_{298}, and ΔG^0_{298}) in kcal mol^{-1} of the Cu$^{+/2+}$-GG, -GGG, and -GGGG Systems and the Cu$^{+/2+}$-glycine System

	species	D_e	D_0	ΔH^0_{298}	ΔG^0_{298}
Cu^+	glycine	75.4[a] (68.1)[b]			
	GG	87.5	85.6	86.4	76.8
	GGG	97.1	95.9	96.5	86.3
	GGGG	104.7	104.4	104.4	97.4
Cu^{2+}	glycine	242.7[a] (214.8)[b]			
	GG	256.4	253.9	255.2	244.2
	GGG	301.7	298.6	300.1	287.5
	GGGG	338.1	335.4	336.8	324.7

[a] Reference 44. [b] Determined at the CCSD(T) level using the B3LYP geometries.

tively. As previously mentioned, the linear dicoordination is very favorable since Pauli repulsion is efficiently reduced through sd σ hybridization, thereby reducing the metal−ligand distance and, thus, increasing the stabilizing electrostatic interaction. Therefore, the interaction energy for the two former systems is not as favorable as for the latter ones. Binding energy of **Cu$^+$-GGGG1** is larger than **Cu$^+$-GGG1** (although both are 180° linearly dicoordinated) because on one hand, the GGGG ligand is more flexible than GGG, which allows shorter metal−ligand distances, and on the other hand, **Cu$^+$-GGGG1** exhibits more Cu−O_{pn} interactions than **Cu$^+$-GGG1** (**O_{p1}** and **O_{p3}** vs **O_{p1}**, respectively). As a consequence, more peptide bonds are strengthened, which contributes to the larger binding energy of the former isomer. In contrast, for the Cu^{2+} systems, the increase in the binding energies is related to the adopted coordination geometry of the most stable isomer. As mentioned, Cu^{2+} dication prefers to saturate its coordination environment. That is, for Cu^{2+}-glycine, the most stable isomer is dicoordinated, for **Cu^{2+}-GG2** tricoordinated, for **Cu^{2+}-GGG1** tetracoordinated, and for **Cu^{2+}-GGGG1** pentacoordinated. Accordingly, it is not surprising to find that the interaction energy follows the order of **Cu^{2+}-GGGG1** > **Cu^{2+}-GGG1** > **Cu^{2+}-GG2**, which is the same than the electrostatic stabilization.

It can be slightly appreciated that the binding energy differences between the "GGGG" and "GGG" forms are smaller than the binding energy differences between the "GGG" and "GG" forms, both in Cu^+- and Cu^{2+}-systems. This fact suggests that for longer peptides than the presented in this work the binding energies will tend to be relatively independent of the length of the peptide.

Conclusions

The coordination properties of the $(glycyl)_n$glycine ($n = 1-3$) oligomers toward the closed-shell $Cu^+(d^{10},{}^1S)$ and the open-shell $Cu^{2+}(d^9,{}^2D)$ metal cations have been analyzed by means of the hybrid B3LYP and BHLYP density functional methods. Results indicate that for Cu^+-$(glycyl)_n$glycine systems the preferred metal coordination follows basically a linear dicoordinated geometry. In particular, for Cu^+-GG, coordination takes place through the amino and the carbonyl groups (**N**,**O**), for Cu^+-GGG, through the oxygen of one amide bond and the carbonyl group (**O_{p1}**,**O**), and for Cu^+-GGGG, through the oxygen of two amide bonds (**O_{p1}**,**O_{p3}**). These results are in very good agreement with a recent X-ray absorption spectroscopy structural study of model Cu(I) peptide complexes, which shows a clear predominance of linear two-coordinated structures.[9] However, for Cu^{2+}-$(glycyl)_n$glycine systems, the metal is coordinated by more than two basic sites, the most stable structures being tricoordinated (**N**,**N_{p1}**,**O**) for Cu^{2+}-GG, tetracoordinated (**N**,**O_{p1}**,**O_{p2}**,**O**) for Cu^{2+}-GGG, and pentacoordinated (**N**,**O_{p1}**,**O_{p2}**,**O_{p3}**,**O**) for Cu^{2+}-GGGG. On the other hand, it is observed that, in contrast to Cu^{2+}-glycine, gas-phase calculations show that the zwitterionic forms[44,46] are quite unstable with respect to the ground-state isomer, probably owing to a noticeable screening effect exerted by large ligands.

Both for Cu^+ and Cu^{2+} metal cations, binding energies increase with the length of the peptide. For Cu^+-containing systems, with a dicoordinated structure in all cases, this enlargement is associated with an efficient reduction of the Pauli repulsion, whereas for Cu^{2+}-containing systems, this is ascribed to an increase of the number of donor atoms coordinating the metal cation. Nevertheless, it can be discerned that for longer $(glycyl)_n$glycyl peptides ($n > 3$) the tendency will probably be to have similar binding energies, as a consequence of a saturated metal environment.

Acknowledgment. Financial support from MCYT and DURSI, through the CTQ2005-08797-C02-02/BQU and SGR2005-00244 projects, and the use of the Catalonia Supercomputer Centre (CESCA) are gratefully acknowledged. A.R. is indebted to the Universitat Autónoma de Barcelona for a doctoral fellowship. E.C. acknowledges the MCYT for a doctoral fellowship.

References and Notes

(1) Mass Spectrometry of Proteins and Peptides. In *Methods of Molecular Biology*; Chapman, J. R., Ed.; Totowa, N. J., 2000; Vol. 146.
(2) Sigel, A.; Sigel, H. Probing of proteins by metal ions and their low-molecular-wieght complexes. In *Metal ions in biological systems*; Marcel Dekker, Inc.: New York, 2001; Vol. 38.
(3) Wilkins, P. C.; Wilkins, R. G. *Inorganic Chemistry in Biology*; Oxford University Press: 1997.
(4) Karr, J. W.; Kaupp, L. J.; Szalai, V. A. *J. Am. Chem. Soc.* **2004**, *126*, 13534.
(5) Hou, L.; Zagorski, M. G. *J. Am. Chem. Soc.* **2006**, *128*, 9260.
(6) Gomez-Balderas, R.; Raffa, D. F.; Rickard, G. A.; Brunelle, P.; Rauk, A. *J. Phys. Chem. A* **2005**, *109*, 5498.
(7) Raffa, D. F.; Gomez-Balderas, R.; Brunelle, P.; Rickard, G. A.; Rauk, A. *J. Biol. Inorg. Chem.* **2005**, *10*, 887.
(8) Marino, T.; Russo, N.; Toscano, M. *J. Phys. Chem. B* **2007**, *111*, 635.
(9) Himes, R. A.; Park, G. Y.; Barry, A. N.; Blackburn, N. J.; Karlin, K. D. *J. Am. Chem. Soc.* **2007**, *129*, 5352.
(10) Tolman, W. B. *J. Biol. Inorg. Chem.* **2006**, *11*, 261.
(11) Luna, A.; Amekraz, B.; Tortajada, J.; Morizur, J. P.; Alcami, M.; Mo, O.; Yanez, M. *J. Am. Chem. Soc.* **1998**, *120*, 5411.
(12) Cerda, B. A.; Hoyau, S.; Ohanessian, G.; Wesdemiotis, C. *J. Am. Chem. Soc.* **1998**, *120*, 2437.
(13) Lee, S.-W.; Kim, H. S.; Beauchamp, J. L. *J. Am. Chem. Soc.* **1998**, *120*, 3188.
(14) Wyttenbach, T.; Bushnell, J. E.; Bowers, M. T. *J. Am. Chem. Soc.* **1998**, *120*, 5098.
(15) Parac, T. N.; Ullmann, G. M.; Kostic, N. M. *J. Am. Chem. Soc.* **1999**, *121*, 3127.
(16) Chu, I. K.; Shoeib, T.; Guo, X.; Rodriquez, C. F.; Hopkinson, A. C.; Siu, K. W. M.; Lau, T. C. *J. Am. Soc. Mass Spectrom.* **2001**, *12*, 163.
(17) Constantino, E.; Rimola, A.; Rodriguez-Santiago, L.; Sodupe, M. *New J. Chem.* **2005**, *29*, 1585.
(18) Kapota, C.; Ohanessian, G. *Phys. Chem. Chem. Phys.* **2005**, *7*, 3744.
(19) Kish, M. M.; Wesdemiotis, C.; Ohanessian, G. *J. Phys. Chem. B* **2004**, *108*, 3086.
(20) Pushie, M. J.; Rauk, A. *J. Biol. Inorg. Chem.* **2003**, *8*, 53.
(21) Shoeib, T.; Rodriquez, C. F.; Michael Siu, K. W.; Hopkinson, A. C. *Phys. Chem. Chem. Phys.* **2001**, *3*, 853.
(22) Wong, C. H. S.; Ma, N. L.; Tsang, C. W. *Chem.−Eur. J.* **2002**, *8*, 4909.
(23) Hattori, T.; Toraishi, T.; Tsuneda, T.; Nagasaki, S.; Tanaka, S. *J. Phys. Chem. A* **2005**, *109*, 10403.
(24) Bauschlicher, C. W.; Ricca, A.; Partridge, H.; Langhoff, S. R. *Recent Advances in Density Functional Theory, Part II*; World Scientific Publishing Co.: Singapore, 1997.
(25) Koch, W.; Holthausen, M. C. *A Chemists's Guide to Density Functional Theory*, 2nd ed.; WILEY-VCH Verlag: Weinheim, Federal Republic of Germany, 2001.
(26) Poater, J.; Sola, M.; Rimola, A.; Rodriguez-Santiago, L.; Sodupe, M. *J. Phys. Chem. A* **2004**, *108*, 6072.

(27) Georgieva, I.; Trendafilova, N.; Rodriguez-Santiago, L.; Sodupe, M. *J. Phys. Chem. A* **2005**, *109*, 5668.
(28) Rimola, A.; Rodríguez-Santiago, L.; Sodupe, M. *J. Phys. Chem. B* **2006**, *110*, 24189.
(29) Sodupe, M.; Bertran, J.; Rodríguez-Santiago, L.; Baerends, E. J. *J. Phys. Chem. A* **1999**, *103*, 166.
(30) Becke, A. D. *J. Chem. Phys.* **1993**, *98*, 5648.
(31) Lee, C.; Yang, W.; Parr, R. G. *Phys. Rev. B* **1988**, *37*, 785.
(32) Becke, A. D. *J. Chem. Phys.* **1993**, *98*, 1372.
(33) Cizek, J. *J. Chem. Phys.* **1966**, *45*, 4256.
(34) Saunders, M.; Houk, K. N.; Wu, Y. D.; Still, W. C.; Lipton, M. J. *J. Am. Chem. Soc.* **1990**, *112*, 1419.
(35) Weiner, S. J.; Kollman, P. A.; Case, D. A.; Singh, U. C.; Ghio, C.; Alagona, G.; Profeta, S., Jr.; Weiner, P. *J. Am. Chem. Soc.* **1984**, *106*, 765.
(36) Weiner, S. J.; Kollman, P. A.; Nguyen, D. T.; Case, D. A. *J. Comput. Chem.* **1986**, *7*, 230.
(37) Mohamadi, F.; Richards, N. G. J.; Guida, W. C.; Liskamp, R.; Lipton, M.; Caufield, C.; Chang, G.; Hendrickson, T.; Still, W. C. *J. Comput. Chem.* **1990**, *11*, 440.
(38) Wachters, A. J. H. *J. Chem. Phys.* **1970**, *52*, 1033.
(39) Hay, P. J. *J. Chem. Phys.* **1977**, *66*, 4377.
(40) Frisch, M. J.; Trucks, G. W.; Schlegel, H. B.; Scuseria, G. E.; Robb, M. A.; Cheesman, J. R.; Montgomery, J. A.; Vreven, T.; Kudin, K. N.; Burant, J. C.; Millam, J. M.; Iyengar, S. S.; Tomasi, J.; Barone, V.; Mennucci, B.; Cossi, M.; Scalmanu, G.; Rega, N.; Petersson, G. A.; Nakatsuji, H.; Hada, M.; Ehara, M.; Toyota, K.; Fukuda, R.; Hasegawa, J.; Ishida, M.; Nakajima, T.; Honda, Y.; Kitao, O.; Nakai, H.; Klene, M.; Li, X.; Knox, J. E.; Hratchian, H. P.; Cross, J. B.; Adamo, C.; Jaramillo, J.; Gomperts, R.; Stratmann, R. E.; Yazyev, O.; Austin, A. J.; Cammi, R.; Pomelli, C.; Ochterski, J. W.; Ayala, P. Y.; Morokuma, K.; Voth, G. A.; Salvador, P.; Dannenberg, J. J.; Zakrzewski, V. G.; Dapprich, S.; Daniels, A. D.; Strain, M. C.; Farkas, O.; Malick, D. K.; Rabuck, A. D.; Raghavachari, K.; Foresman, J. B.; Ortiz, J. V.; Cui, Q.; Baboul, A. G.; Clifford, S.; Cioslowski, J.; Stefanov, B. B.; Liu, G.; Liashenko, A.; Piskorz, P.; Komaromi, I.; Martin, R. L.; Fox, D. J.; Keith, T.; Al-Laham, M. A.; Peng, C. Y.; Nanayakkara, A.; Challacombe, M.; Gill, P. M. W.; Johnson, B.; Chen, W.; Wong, M. W.; Gonzalez, C.; Pople, J. A. *Gaussian 03*; Gaussian Inc.: Wallingford, CT, 2004.
(41) McQuarrie, D. *Statistical Mechanics*; Harper and Row: New York, 1986.
(42) Weinhold, F.; Carpenter, J. E. *The Structure of Small Molecules and Ions*; Plenum: New York, 1988.
(43) Gil, A.; Bertran, J.; Sodupe, M. *J. Chem. Phys.* **2006**, *124*, 154306.
(44) Bertran, J.; Rodriguez-Santiago, L.; Sodupe, M. *J. Phys. Chem. B* **1999**, *103*, 2310.
(45) Noguera, M.; Bertran, J.; Sodupe, M. *J. Phys. Chem. A* **2004**, *108*, 333.
(46) Pulkkinen, S.; Noguera, M.; Rodríguez-Santiago, L.; Sodupe, M.; Bertrán, J. *Chem.−Eur. J.* **2000**, *6*, 4393.